

See discussions, stats, and author profiles for this publication at: <https://www.researchgate.net/publication/231375389>

Formulation Affects the Rate of Membrane Degradation Catalyzed by Cationic Amphiphilic Drugs

ARTICLE in INDUSTRIAL & ENGINEERING CHEMISTRY RESEARCH · DECEMBER 2007

Impact Factor: 2.59 · DOI: 10.1021/ie071265q

CITATIONS

10

READS

26

6 AUTHORS, INCLUDING:



Duncan Casey

Liverpool John Moores University

12 PUBLICATIONS 120 CITATIONS

SEE PROFILE



Rob V. Law

Imperial College London

128 PUBLICATIONS 1,942 CITATIONS

SEE PROFILE



Richard H Templer

Imperial College London

129 PUBLICATIONS 6,119 CITATIONS

SEE PROFILE

Formulation Affects the Rate of Membrane Degradation Catalyzed by Cationic Amphiphilic Drugs

Duncan R. Casey,[†] Sarra C. Sebai,[†] Gemma C. Shearman, Oscar Ces, Robert V. Law, and Richard H. Templer*

Chemical Biology Centre, Department of Chemistry, Imperial College London, South Kensington Campus, London SW7 2AZ, United Kingdom

Antony D. Gee

GSK Clinical Imaging Centre, Imperial College London, Hammersmith Hospital, Du Cane Road, London W12 0NN, United Kingdom

Cationic amphiphilic drugs (CADs), such as haloperidol, are able to translocate through biological membrane bilayers via a chemically activated degradation of the phospholipid fabric of the membrane, which may constitute a third type of drug translocation process. We present evidence that this effect is dependent on the drug formulation. The choice of drug counterion is shown to influence the rate of bilayer hydrolysis, leading either to promotion of the reaction or the drug's precipitation via a counterion condensation process.

Introduction

The transport of compounds, pharmaceutical or otherwise, across a cell membrane is conventionally split into one of two mechanisms: either passive transport or active transport.^{1–3} Active transport is dominated by those compounds, such as glucose and insulin, that are recognized as being essential by specific biological receptors. These are pumped from systemic circulation into tissue and against the concentration gradient, at the cost of cellular energy in the form of adenosine triphosphate.⁴ Passive transport, by contrast, requires no such expenditure of cellular energy and, thus, is considered to proceed via a diffusive mechanism, which fits well with the experimental data.^{5–7} Passive diffusion can occur in both directions across a membrane, although the net direction is for molecules to travel down the concentration gradient. The rate of diffusion is governed by Fick's First Law of Diffusion, with the rate of diffusion being proportional to the concentration gradient across the membrane.

Despite the apparent prevalence of passive diffusion as a transportation mechanism *in vivo*, relatively little research has been undertaken regarding its physical underpinnings. This is of critical importance, given that the majority of pharmaceutical compounds are hydrophobic (they have an octanol:water partition coefficient ($\log P$) value in the range of 3–5, and molecules with a $\log P$ value of >5 have been shown empirically to have a low bioavailability⁸). Despite this, they seem to readily diffuse into and across aqueous cellular compartments, through their preferred environment into regions in which their presence is energetically unfavorable.

A range of studies on highly hydrophobic compounds such as lipid signaling molecules^{9–12} and cannabinoids^{13–15} have suggested that current transport models may not be all-encompassing. In these investigations, the compounds are shown to migrate to the lipophilic membrane region, then diffuse laterally through it to reach receptor binding sites. It was this transport mechanism that, until recently, led to the incorrect assumption that many receptors were expressed on the outer

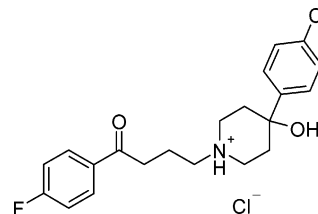


Figure 1. Structure of haloperidol·HCl, which is a typical cationic amphiphilic drug (CAD).

bilayer leaflet. The cannabinoids have $\log P$ values in the range of 7–8, which implies very low solubility in water. Even a drug such as haloperidol (Figure 1), with a $\log P$ value of 4.2, will partition into lipophilic media to the extent that only $\sim 0.1\%$ will be available for systemic circulation (studies indicate that, for monovalent cationic drugs at pH 7.4, octanol:water and phosphatidylcholine lipid:water partition coefficients are very similar¹⁶). In both cases, it is unclear how the molecules are able to translocate from one bilayer to the next, given that, once inserted in the hydrophobic part of the bilayer, it is energetically unfavorable for them to leave. However, bilayer translocation must be occurring, because haloperidol exhibits an acceptable pharmacokinetic profile, being very widely prescribed as an anti-psychotic drug. This implies that the interactions between systemic ligands and cellular receptors may be more complex than envisaged by the traditional “lock and key” model. More importantly, it also suggests the action of a transport mechanism other than active transport and passive diffusion, which are normally ascribed to these and other, less-hydrophobic drugs.

In a previous study,¹⁷ it was demonstrated that a range of cationic amphiphilic drugs (CADs) such as haloperidol could catalyze the hydrolysis of ester linkages within membranes composed of phospholipids such as dioleoylphosphatidylcholine, (DOPC), thereby releasing lyso-lipids (in this case, mono-oleoylphosphatidylcholine (lyso-PC)) and the concomitant fatty acid, oleic acid (OA). Over a wide range of temperatures, DOPC, when mixed with water, will form a fluid lamellar structure.¹⁸ In contrast, lyso-PC forms micellar aggregates with an interface that curves strongly away from the aqueous interface, whereas OA/DOPC mixtures exhibit a strong propensity for interfacial curvature toward the water, forming an

* To whom correspondence should be addressed. E-mail address: o.ces@imperial.ac.uk.

[†] Joint first authorship.

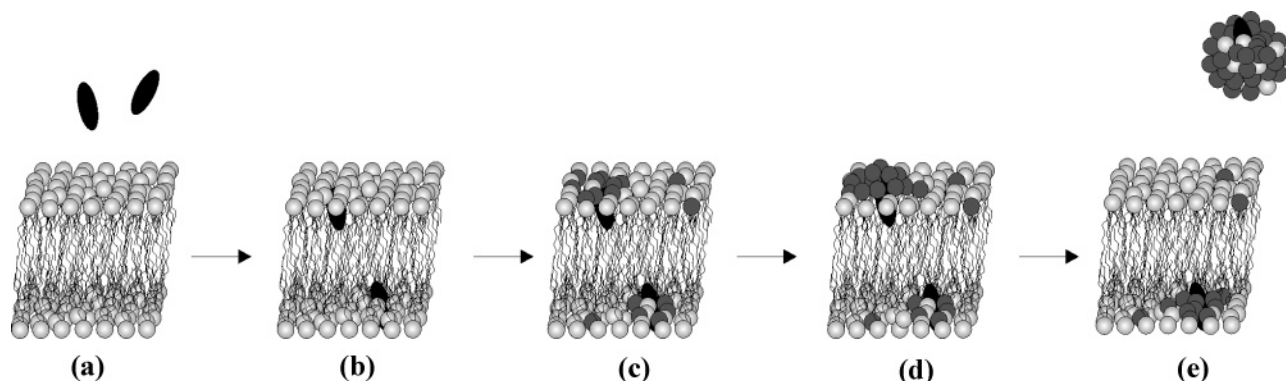


Figure 2. Schematic depicting the proposed mechanism of drug transport: (a) the drugs, shown as black ovoids, are introduced to a DOPC bilayer (where the lipids are depicted as light gray objects), (b) to which they bind; (c) CAD-catalyzed hydrolysis of DOPC leads to the formation of lyso-PC (dark gray regions); (d) over time, lyso-PC accumulates; and (e) as the concentration of lyso-PC increases, micelles will bud off. Incorporation of the drug molecules within the micelles and subsequent binding to a different membrane leaflet results in drug translocation.

inverse hexagonal phase when sufficient OA is present.^{19,20} Van Etcheld et al. have shown that lyso-PC phase separates from DOPC at sufficiently high concentrations²¹ to form micelles, and previous experiments have shown that CADs cause the release of lyso-PC leaving OA-enriched DOPC.¹⁷

The postulated mechanism of this membrane degradation phenomenon is based on an acid-catalyzed ester hydrolysis reaction, which is triggered by the introduction of a proton from the weakly acidic quaternary amine formed by CADs at a physiological pH value. Rotational-echo double-resonance nuclear magnetic resonance (NMR)²² data have shown that the orientation and depth of cannabinoids and a range of common amphiphilic drugs locates their charged and/or polar regions at the membrane interface, within a few angstroms of the ester moieties of PC.^{23,24} Experiments with ether-linked phospholipids have shown no similar activity, because an ether moiety cannot be hydrolyzed in the same manner.¹⁷

There are several articles in the literature describing phenomena in systems similar to those described here, which may be attributable to the downstream effects of this hydrolysis: for example, the erosion of PC-rich microdomains has been analyzed using atomic force microscopy,^{25,26} and Langmuir studies have revealed that the addition of CADs such as chlorpromazine dramatically increases the area of a monolayer containing diacyl lipids.²⁷ However, the previous study was the first to propose a common cause of these effects and successfully isolate the predicted degradation products from such a system.

Using a commercially available fluorescence-labeled CAD, it was demonstrated that the membrane fragments created by this reaction contained significant quantities of the administered drug.¹⁷ In this way, the largely hydrophobic drug is encapsulated by the membrane fragments formed from the lipid degradation products, thus solubilizing it in water, as shown in Figure 2. Furthermore, these membrane fragments can subsequently fuse with the membranes of surrounding vesicles, effectively transporting their cargoes of drug molecules into a fresh system, allowing the catalytic cycle to begin again. The reaction could, in theory, be triggered by any amphiphile of the correct dimensions with the ability to carry a proton. The CAD is responsible for delivering a proton sufficiently close to the acyl groups of a neighboring lipid to allow it to react: there is no covalent bond formed between the drug and its target lipid.

Because the lamellar bilayers formed by pure DOPC in solution are a close analogue of biological membranes,^{28,29} it was proposed that this process constitutes a third drug translocation mechanism. Strong drug-lipid interactions have previ-

ously been demonstrated via NMR experiments²³ and, indeed, migration of CADs to membrane interfaces has been observed to occur within <150 ms.¹⁷ Further studies (unpublished data from S. Sebai and R. Ling) undertaken using the fluorescein-tagged phosphatidylethanolamine lipids first used by O'Shea et al.^{30,31} demonstrated that, at physiologically relevant concentrations, the movement of the CAD molecules to the lipid/water interface was more rapid than could be accurately measured under those experimental conditions.

Previous studies have shown that the rate and degree of binding of amphiphiles to a membrane is dependent on its mechanical properties.³² The intercalation of CADs or other small, planar amphiphilic molecules between such stressed membrane components can relieve the stored curvature elastic stress within the membrane³³ and is thus associated with a drop in the overall free energy of the system. This promotes their incorporation, which further increases the rate of degradation. This was demonstrated in the previous study, where saturated lipids with shorter acyl chains (and, hence, reduced stored curvature elastic stress) displayed much lower rates of hydrolysis.¹⁷

The regulation of such a hydrolytic process via structural alteration of a drug may be possible and investigations are ongoing; however, in some instances, the chemical modifications necessary may prove to be incompatible with the specificity profiles of any given pharmacophore. By contrast, alterations in drug formulation may present a relatively simple, safe, and robust method for increasing or decreasing the aqueous solubility of a compound, altering its log *P* value and, thus, its effects on the surrounding cell membranes.

The most accessible route for modification of CADs lies with the choice of salt form. Haloperidol, for example, is typically supplied as a hydrochloride; however, studies have suggested that its poor aqueous solubility can be dramatically improved by substituting this for a mesylate or, to a lesser extent, a phosphate, even under physiologically relevant buffer conditions.^{34,35} This suggests that the drug is associated with its original counterion for a significant period, even in the presence of excess chloride, indicating the possibility of a long-lived tight ion-binding pair.

The interactions between ions and their environment have long been studied by chemists. An example of such a study led to the Hofmeister series, which is an empirical list that relates the ability of an added ion to cause a mixture of hen egg-white proteins to precipitate from aqueous solution.³⁶

Experimental Methods

Unless otherwise stated, all chemicals were obtained from Sigma–Aldrich (U.K.). Trifluoroacetic acid and methanesulfonic acid were purchased from ABCR (Germany). DOPC was purchased from Avanti Polar Lipids (USA) as a lyophilized powder for small-angle X-ray scattering experiments (SAXS), NMR studies, and high-pressure liquid chromatography (HPLC) analysis. All chemicals were of reagent grade or better and were used without further purification.

HPLC analysis was performed with a dual-pump system (Model 626 LC, Waters). Measurements were conducted on a Kromasil 60-5 column (Hi-Chrom) and analyzed via evaporative light scattering, using an ESA 301 detector. The mobile phase gradient ran from 101/21/2/0.1 hexane/iso-propyl alcohol/acetic acid/triethylamine w/w to 155:17.5:2:0.1 iso-propyl alcohol/water/acetic acid/triethylamine.

SAXS experiments were conducted using a custom-designed beamline, based around a Bede Microsource X-ray generator (Durham, U.K.) with integrated optics, an Ealing linear transition stage (Ealing Electro Optics, U.K.), and a Photonic Science, Ltd., Gemstar intensified CCD X-ray detector (Battle, U.K.). X-ray exposures (5×60 s at 25°C) were combined to give a cumulative diffraction plot. The resulting diffraction patterns were analyzed with the IDL-based AXcess software package that was developed by Andrew Heron at Imperial College.

Synthesis. (1) Haloperidol·HCl.³⁷ One hundred milligrams ($250\ \mu\text{mol}$) of haloperidol (free base) was dissolved in 8 mL of isopropyl alcohol, 8 mL of 12 M HCl, and 4 mL of acetone. The mixture was stirred at room temperature for 10 min, and the solvents were then removed under reduced pressure. The product was a quantitative yield of white crystals with the following specifications: melting point (T_m) = $223\text{--}224^\circ\text{C}$, δ [^1H , 270 MHz, d_6 -DMSO]: 1.68 (m, 2H); 1.95 (m, 2H); 2.29 (m, 2H); 3.18 (m, 8H); 5.46 (s, 1H); 7.28 (m, 6H); 7.93 (m, 2H); 10.27 (broad, 1H).

(2) Haloperidol·HBr. Similar to haloperidol·HCl, but with aqueous HBr. $T_m = 154^\circ\text{C}$. NMR showed a dimeric salt structure.³⁸ δ [^1H , 270 MHz, d_6 -DMSO]: 1.44 (d, 1H); 1.92 (m, 1H); 2.19 (m, 2H); 2.38 (m, 1H); 2.90 (m, 1H); 3.35 (m, 6H); 3.52 (m, 2H); 5.71 (m, 0.5H); 6.34 (m, 0.5H); 7.58 (m, 6H); 8.19 (m, 2H); 9.43 (broad, 0.5H); 9.76 (m, 0.5H).

(3) Haloperidol·CH₃SO₃H (mesylate). The mesylate salt was successfully prepared via the addition of 12 mg ($125\ \mu\text{mol}$) of methanesulfonic acid to a solution of 50 mg ($125\ \mu\text{mol}$) of haloperidol in 5 mL of tetrahydrofuran (THF), which was then stirred for 1 h at room temperature. Solvents were evaporated under reduced pressure to yield 57.0 mg ($120.8\ \mu\text{mol}$, 96.6% yield) of white crystals. δ [^1H , 270 MHz, CDCl_3]: 1.90 (m, 2H); 2.16 (m, 2H); 2.49 (m, 2H); 2.62 (s, 3H); 3.04 (m, 4H); 3.32 (m, 4H); 4.41 (broad s, 2H); 7.13 (m, 4H); 7.42 (m, 2H); 9.68 (broad s, 1H).

(4) Haloperidol·HCO₂H (formate). Similar to haloperidol·HCl, but with 99.7% formic acid. $T_m = 132^\circ\text{C}$. δ [^1H , 400 MHz, d_6 -DMSO]: 1.49 (d, 2H); 1.84, (m, 4H); 2.18 (m, 4H + DMSO); 4.10 (broad, 1H + H₂O); 7.44 (m, 6H); 8.06 (m, 2H); 8.20 (broad s, 1H).

(5) Haloperidol·F₃CCO₂H (TFA). Fifty milligrams ($125\ \mu\text{mol}$) of haloperidol was dissolved in 5 mL of a 1:1 trifluoroacetic acid (TFA)/dichloromethane (DCM) mixture and stirred for 1 h at room temperature. Solvents were removed under reduced pressure to give a quantitative yield of colorless gum. δ [^1H , 270 MHz, CDCl_3]: 1.85 (m, 2H); 2.02 (m, 2H); 2.36 (m, 2H); 3.08 (t, 4H); 3.27 (dd, 2H); 3.39 (m, 2H); 5.14 (m, 1H + DCM); 7.20 (m, 6H); 7.89 (m, 2H); 11.12 (broad s, 1H).

(6) Haloperidol· $\frac{1}{2}\text{HO}_2\text{CCHCHCO}_2\text{H}$ (maleate). The maleate salt was successfully prepared as haloperidol mesylate. $T_m = 131\text{--}133^\circ\text{C}$. δ [^1H , 400 MHz, d_6 -DMSO]: 1.89 (d, 2H); 2.13 (m, 2H); 2.28 (m, 2H); 2.91 (t, 2H); 3.18 (m, 4H); 3.22 (d, 2H); 6.14 (s, 1H); 7.13 (t, 2H); 7.28 (t, 2H); 7.40 (d, 2H); 7.95 (m, 2H).

Sample Preparation for HPLC and SAXS. Twenty five milligrams ($32\ \mu\text{mol}$) of lipid was dissolved in dry cyclohexane and lyophilized under liquid nitrogen. The dry powder was redissolved in 0.5 mL of a 1:1 chloroform/methanol mixture and dispersed in a sample vial that contained $1.6\ \mu\text{mol}$ of haloperidol salt. This mixture was subjected to a vortex for 1 min, dried under a nitrogen stream until a translucent film was observed, and then left to desiccate in a vacuum oven at 37°C overnight.

The dry lipid–haloperidol salt mixture was hydrated with $75\ \mu\text{L}$ of 10 mM Tris buffer (pH 7.4–3:1 buffer/lipid, w/w). The hydrated sample was subjected to a vortex for 30 s before being centrifuged at 3000 rpm for 30 s. The process was repeated three times, to ensure that the sample was homogeneous. The vial was sealed and placed in an aluminum heating block within a dark oven to incubate at 37°C . Sample hydration levels were monitored over the course of each experiment. This process was applied to each of the haloperidol salt forms, a haloperidol-free base, and a control vessel that contained only DOPC. An additional vessel that contained haloperidol·HCl was prepared for SAXS analysis.

Samples with a volume of $8\ \mu\text{L}$ were removed from each of the vials at regular periods over the following 8 days. Each sample was frozen in liquid nitrogen, dried under vacuum, and then redissolved in 1 mL of a mobile phase and analyzed via HPLC.

Samples with a volume of $10\ \mu\text{L}$ were removed from the bulk haloperidol·HCl sample on days 1, 5, and 7 and analyzed via SAXS. The samples were dispersed in 1.5-mm-diameter glass capillary tubes before being flame-sealed, the end of which was then coated in a silicone sealant (Dow Corning Corp.).

Results and Discussion

Effects of Counterions on CAD-Catalyzed Membrane Degradation. Time-dependent HPLC analysis was undertaken on DOPC:haloperidol samples in the presence of TFA, formate, maleate, and hydrochloride counterions. Only monovalent counterions were studied, which confined the experiment to the study of the more-chaotropic salt forms. These preferentially reside at the interface rather than in the bulk solution, inhibiting the hydrolysis. DOPC degradation and lyso-PC appearance profiles for these samples constructed using HPLC analysis are shown in Figure 3. Significant DOPC hydrolysis was detected in both the haloperidol formate (the most kosmotropic of the ions studied) and haloperidol TFA samples, as shown in Figure 3a; the rates of degradation in the hydrochloride and maleate systems are indistinguishable from the background. Note that these measurements were conducted on condensed-phase systems, thereby reducing the rate of reaction, with respect to measurements conducted in vesicular environments.

Previous work has demonstrated that the hydrolytic activity of amphipathic CAD molecules at membrane interfaces is sensitive to the degree of stored curvature elastic stress in the bilayer.¹⁷ This strain occurs due to the propensity for each monolayer leaflet in the bilayer to bend in equal but opposite directions. In a flat bilayer, this is physically frustrated and causes the stored curvature elastic stress. We can understand the effect at the molecular level by considering a flat monolayer

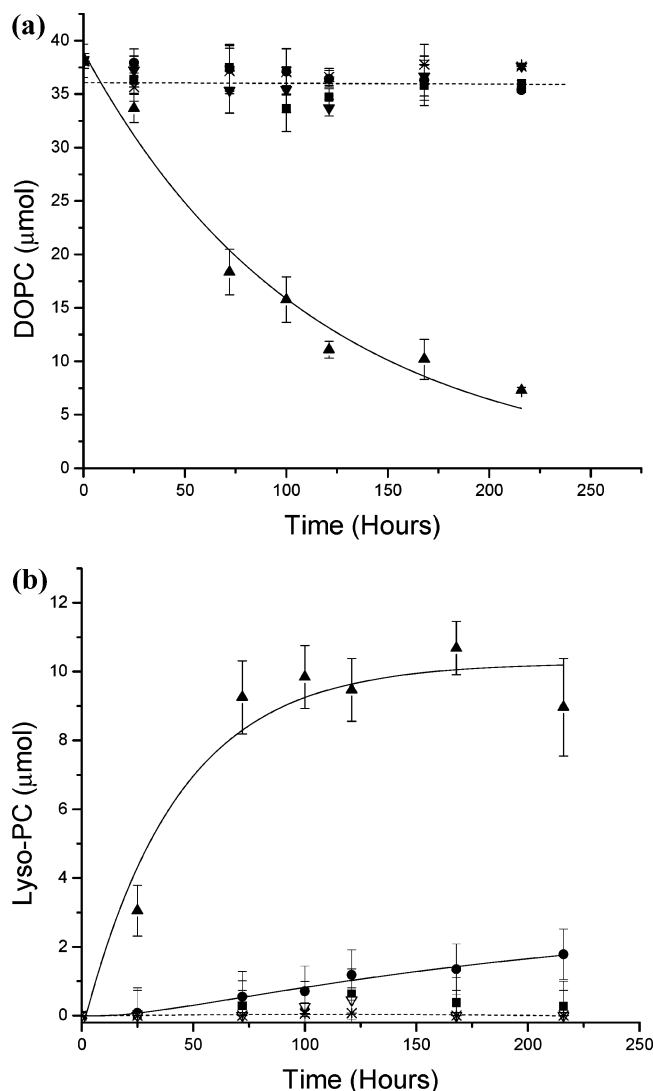


Figure 3. (a) DOPC degradation and (b) lyso-PC emergence profiles resulting from the hydrolysis of DOPC:haloperidol systems in the presence of (▲) TFA, (●) formate, (*) maleate, and (■) hydrochloride counterions, plus (▽) the control sample. A guide for the eye has been applied to the experimental curves. The dashed line represents the maleate and hydrochloride counterions.

that is composed of lipids where the cross-sectional area of the chain is compressed and the headgroup area is expanded. Here, the monolayer would reduce its curvature elastic energy by bending toward the water, because this would reduce the headgroup area while simultaneously expanding the cross-sectional area of the chain. The insertion of a drug molecule at

the polar/apolar interface in such a case will reduce the stored curvature elastic stress (because it allows the chain area to increase). The single-chain lipid (lyso-PC) has a strong tendency to create interfaces that bend away from the water, whereas oleic acid/DOPC mixtures have a strong tendency to bend toward the water; therefore, one would expect the local distribution of the products of hydrolysis to have an effect on hydrolysis rates.

During the hydrolysis phenomena monitored in Figure 3, the composition of the membrane varies as a function of time (DOPC is degraded to OA and lyso-PC), as does the ratio of lyso-PC in micelles ($N_{\text{Lyso-M}}$) to that in the bilayer components ($N_{\text{Lyso-B}}$). This makes modeling the kinetics of the process extremely difficult, as the stored curvature elastic stress, which regulates the rate of reaction, is not a time-independent constant. The rates of the similar reaction mediated by phospholipase A₂ ((PLA₂)) have been investigated in some detail.^{39,40} Some studies indicate that the activity of the enzyme is strongly linked to the relatively slow formation of acid-rich anionic microdomains, which leads to “lag-burst” kinetics.^{41–43} It may prove that a similar effect is at work in this model, and that the observed plateau of lyso-PC levels is simply a transitional state; however, this seems unlikely, given that, unlike PLA₂, the drugs under investigation are capable of hydrolyzing either or both of the lipids’ acyl chains. Interestingly, previous studies have demonstrated that a range of CAD molecules are capable of inhibiting the action of PLA₂, which suggests that some type of negative feedback process may be at work.^{44,45} Although it has been possible to measure the total DOPC and lyso-PC content ($N_{\text{Lyso-M}} + N_{\text{Lyso-B}}$) of the samples, as a function of time, the data do not allow us to discriminate between the sub-mesophase fractions $N_{\text{Lyso-M}}$ and $N_{\text{Lyso-B}}$. Moreover, there are currently no models that allow us to quantify the stored curvature elastic stress as a function of composition in ternary mixtures of OA, lyso-PC, and DOPC.

Our results also suggest that, if membrane hydrolysis is to be observed, ion recondensation and precipitation must be avoided. This hypothesis was supported by SAXS studies conducted in parallel with the HPLC experiments. Figure 4 depicts the SAXS patterns recorded for a DOPC:haloperidol·HCl (20:1) sample, as a function of time.

The presence of the protonated haloperidol at the membrane interface, which is key to the bilayer hydrolysis, promotes the formation of a swollen fluid lamellar L_α phase, the *d*-spacing of which increased to a maximum of 107.71 Å after five days (see Figure 4b). This swelling, which is not observed in the fluid lamellar phase formed by the control sample (*d*-spacing of 61.3 Å) is the result of repulsion between charged bilayer interfaces.⁴⁶ After eight days, the *d*-spacing of the DOPC:haloperidol·HCl system was observed to have decreased to 89.46

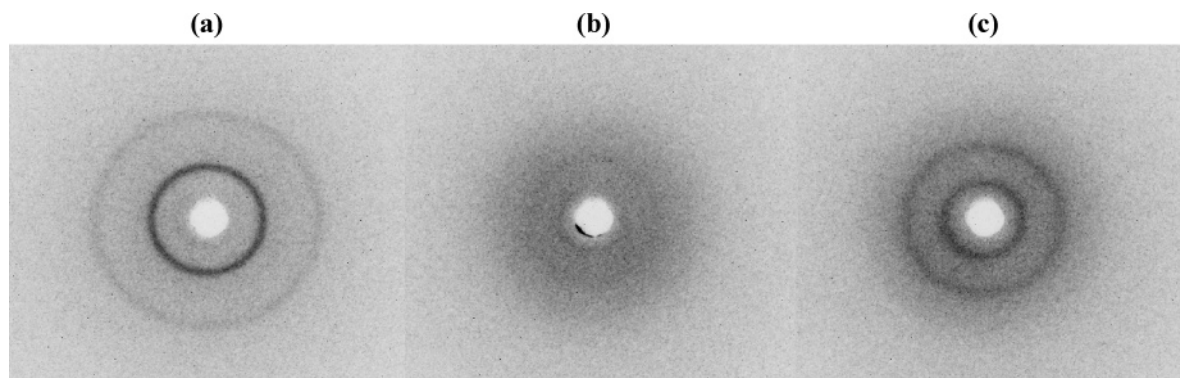


Figure 4. Small-angle X-ray scattering (SAXS) images showing the swelling of an L_α DOPC system through the addition of haloperidol: (a) DOPC in excess water (61.36 ± 0.57 Å), (b) five days after the addition of haloperidol (107.70 ± 3.21 Å), and (c) eight days (89.46 ± 1.07 Å).

Å (see Figure 4c). Further investigations at room temperature showed that a more-pronounced decrease in repeat spacing occurred in DOPC:haloperidol·HCl systems after several weeks, with a minimum *d*-spacing of 56 Å (data not shown). This is markedly lower than that of a pure DOPC fluid lamellar phase under excess water conditions, which is what would be expected in this instance and implies that the lamellar phase has been dehydrated.

At this point, the drug no longer resides at the bilayer interface and, instead, precipitates to form drug crystals, halting the hydrolysis reaction in the process. Furthermore, this shrinkage represents a significant loss of water from the aqueous channels between bilayers in the condensed-phase system, induced either by the condensation of anions to the membrane surface or by the act of crystallization itself. Because of the low rate of reaction in the DOPC:haloperidol·HCl systems, the variation in the lattice parameter is unlikely to be the result of modifications to the membrane composition brought about by membrane hydrolysis that, in turn, modify biophysical parameters such as the bending rigidity. Precipitation of haloperidol crystals was also confirmed by microscopy studies (data not shown). In contrast to these results, the DOPC:haloperidol formate and DOPC:haloperidol TFA samples showed no such crystal formation. As mentioned previously, significant degradation above that of the control was noted only in the TFA and formate samples. This implies that, in the other instances, either the drug is inactive in certain forms or, as suggested by microscopy studies, the drug precipitated from solution altogether to form a crystalline deposit on the vial.

Conclusions

Our experiments demonstrate that the choice of counterion exerts a major effect on the hydrolytic activity of haloperidol and regulates the possibility of charge recondensation phenomena, which will reduce the membrane:water partition coefficient and ultimately result in precipitation of the drug molecule. Despite the excess of Cl[−] ions in these experiments, altering the counterion resulted in dramatic differences in the activity of haloperidol within the bilayer. These results imply that the choice of counterion may have a significant effect on the ability of cationic amphiphilic drug molecules to hydrolyze membrane systems and, therefore, their ability to traverse bilayer scaffolds via a degradative mechanism. In instances where this pathway is inhibited, transport across a phospholipid bilayer is restricted to the mode of passive (and active if under *in vivo* conditions) transport. These results imply that variations in the nature of the associated anion may allow the “tuning” of a pharmacophore’s systemic mobility without compromising or even modifying its structure. Currently, variations in drug formulations, with respect to the nature of the associated anion, are undertaken to maximize the stability of the cationic amphiphilic drug (CAD) in solution; such formulations may not, in fact, be optimal, with respect to the mobility of the drug *in vivo* and, therefore, its ability to reach its intended target. Finally, the extent of hydrolysis confirmed that the mechanism must be catalytic, with respect to haloperidol, because the extent of degradation exceeded that which could be attributed to a stoichiometric reaction.

Acknowledgment

We thank GSK plc. and the Chemical Biology Doctoral Training Centre (Imperial College London, EPSRC Award Nos. GR/S47144/01 and EP/E50163X/1) for funding SCS and DC and the UK Engineering and Physical Research Council (EPSRC) for the Award of Platform Grant No. GR/S77721.

Literature Cited

- (1) Davson, H.; Danielli, J. F. *Permeability of Natural Membranes*, 2nd Edition; Macmillan: New York, 1952.
- (2) Zwolinski, B. J.; Eyring, H.; Reese, C. E. Diffusion and Membrane Permeability. I. *J. Phys. Chem.* **1949**, *53* (9), 1426–1453.
- (3) Collander, R. The Permeability of Plant Protoplasts to Small Molecules. *Physiol. Plant.* **1949**, *2* (4), 300–311.
- (4) Alvarado, F. Transport of Sugars and Amino Acids in the Intestine: Evidence for a Common Carrier. *Science* **1966**, *151* (3713), 1010–1013.
- (5) Wright, L. L.; Painter, G. R. Role of desolvation energy in the nonfacilitated membrane permeability of dideoxyribose analogs of thymidine. *Mol. Pharmacol.* **1992**, *41* (5), 957–962.
- (6) Domin, B. A.; Mahony, W. B.; Koszalka, G. W.; Porter, D. J.; Hajian, G.; Zimmerman, T. P. Membrane permeation characteristics of 5′-modified thymidine analogs. *Mol. Pharmacol.* **1992**, *41* (5), 950–956.
- (7) Kamp, F.; Kizilbash, N.; Corkey, B. E.; Berggren, P.-O.; Hamilton, J. A. Sulfonyleureas Rapidly Cross Phospholipid Bilayer Membranes by a Free-Diffusion Mechanism. *Diabetes* **2003**, *52* (10), 2526–2531.
- (8) Lipinski, C. A.; Lombardo, F.; Dominy, B. W.; Feeney, P. J. Experimental and computational approaches to estimate solubility and permeability in drug discovery and development settings. *Adv. Drug Delivery Rev.* **1997**, *23* (1–3), 3–25.
- (9) Kabarowski, J. H. S.; Xu, Y.; Witte, O. N. Lysophosphatidylcholine as a ligand for immunoregulation. *Biochem. Pharmacol.* **2002**, *64* (2), 161–167.
- (10) Murakami, N.; Yokomizo, T.; Okuno, T.; Shimizu, T. G2A is a Proton-sensing G-protein-coupled Receptor Antagonized by Lysophosphatidylcholine. *J. Biol. Chem.* **2004**, *279* (41), 42484–42491.
- (11) Qiao, J.; Huang, F.; Naikawadi, R. P.; Kim, K. S.; Said, T.; Lum, H. Lysophosphatidylcholine impairs endothelial barrier function through the G protein-coupled receptor GPR4. *Am. J. Physiol.* **2006**, *291* (1), L91–L101.
- (12) Xu, Y. Sphingosylphosphorylcholine and lysophosphatidylcholine: G protein-coupled receptors and receptor-mediated signal transduction. *Biochim. Biophys. Acta* **2002**, *1582* (1–3), 81–88.
- (13) Guo, J.; Pavlopoulos, S.; Tian, X.; Lu, D.; Nikas, S. P.; Yang, D. P.; Makriyannis, A. Conformational Study of Lipophilic Ligands in Phospholipid Model Membrane Systems by Solution NMR. *J. Med. Chem.* **2003**, *46* (23), 4838–4846.
- (14) Tian, X.; Guo, J.; Yao, F.; Yang, D.-P.; Makriyannis, A., The Conformation, Location, and Dynamic Properties of the Endocannabinoid Ligand Anandamide in a Membrane Bilayer. *J. Biol. Chem.* **2005**, *280* (33), 29788–29795.
- (15) Makriyannis, A.; Tian, X.; Guo, J. How lipophilic cannabinergic ligands reach their receptor sites. *Prost. Lip. Med.* **2005**, *77* (1–4), 210–218.
- (16) Lullmann, H.; Wehling, M. The binding of drugs to different polar lipids *in vitro*. *Biochem. Pharmacol.* **1979**, *28* (23), 3409–3415.
- (17) Baci, M.; Sebai, S. C.; Ces, O.; Mulet, X.; Clarke, J. A.; Shearman, G. C.; Law, R. V.; Templer, R. H.; Plisson, C.; Parker, C. A.; Gee, A. Degradative transport of cationic amphiphilic drugs across phospholipid bilayers. *Philos. Trans. R. Soc. London. A* **2006**, *364* (1847), 2597–2614.
- (18) Leonenko, Z. V.; Finot, E.; Ma, H.; Dahms, T. E. S.; Cramb, D. T. Investigation of Temperature-Induced Phase Transitions in DOPC and DPPC Phospholipid Bilayers Using Temperature-Controlled Scanning Force Microscopy. *Biophys. J.* **2004**, *86* (6), 3783–3793.
- (19) Bergstrand, N.; Edwards, K. Aggregate Structure in Dilute Aqueous Dispersions of Phospholipids, Fatty Acids, and Lysophospholipids. *Langmuir* **2001**, *17* (11), 3245–3253.
- (20) Brentel, I.; Arvidson, G.; Lindblom, G., Phase equilibria of the ternary system 1-palmitoyl-*sn*-glycero-3-phosphocholine/oleic acid/water studied by NMR. *Biochim. Biophys. Acta* **1987**, *904* (2), 401–404.
- (21) Van Echteld, C. J. A.; De Kruijff, B.; Mandersloot, J. G.; De Gier, J. Effects of lysophosphatidylcholines on phosphatidylcholine and phosphatidylcholine/cholesterol liposome systems as revealed by ³¹P-NMR, electron microscopy and permeability studies. *Biochim. Biophys. Acta* **1981**, *649*, 211–220.
- (22) Gullion, T.; Schaeffer, J., Rotational-Echo Double-Resonance NMR. *J. Magn. Reson.* **1989**, *81*, 196–200.
- (23) Seydel, J. K.; Wassermann, O. NMR-Studies on the molecular basis of drug-induced phospholipidosis—II. Interaction between several amphiphilic drugs and phospholipids. *Biochem. Pharmacol.* **1976**, *25* (21), 2357–2364.
- (24) Yang, D.-P.; Banijamali, A.; Charalambous, A.; Marciniak, G.; Makriyannis, A. Solid state ²H-NMR as a method for determining the orientation of cannabinoid analogs in membranes. *Pharmacol., Biochem. Behav.* **1991**, *40* (3), 553–557.

- (25) Berquand, A.; Mingeot-Leclercq, M. P.; Dufrene, Y. F. Real-time imaging of drug-membrane interactions by atomic force microscopy. *Biochim. Biophys. Acta* **2004**, *1664* (2), 198–205.
- (26) Tyteca, D.; Schanck, A.; Dufrene, Y. F.; Deleu, M.; Courtoy, P. J.; Tulkens, P. M.; Mingeot-Leclercq, M. P. The Macrolide Antibiotic Azithromycin Interacts with Lipids and Affects Membrane Organization and Fluidity: Studies on Langmuir-Blodgett Monolayers, Liposomes and J774 Macrophages. *J. Membr. Biol.* **2003**, *192* (3), 203–215.
- (27) Agasosler, A. V.; Tungodden, L. M.; Cejka, D.; Bakstad, E.; Sydnnes, L. K.; Holmsen, H. Chlorpromazine-induced increase in dipalmitoylphosphatidylserine surface area in monolayers at room temperature. *Biochem. Pharmacol.* **2001**, *61* (7), 817–825.
- (28) Sessa, G.; Weissmann, G. Phospholipid spherules (liposomes) as a model for biological membranes. *J. Lipid Res.* **1968**, *9* (3), 310–318.
- (29) Wohnsland, F.; Faller, B. High-throughput permeability pH profile and high-throughput alkane/water log *P* with artificial membranes. *J. Med. Chem.* **2001**, *44* (6), 923–30.
- (30) Wall, J.; Ayoub, F.; O'Shea, P. Interactions of macromolecules with the mammalian cell surface. *J. Cell Sci.* **1995**, *108* (7), 2673–2682.
- (31) Cladera, J.; O'Shea, P. Generic techniques for fluorescence measurements of protein-ligand interactions; real-time kinetics & spatial imaging. In *Protein-Ligand Interactions*; Harding, S. E., Chowdery, B., Eds.; Oxford University Press: Oxford, U.K., 2001; pp 169–200.
- (32) Attard, G. S.; Templer, R. H.; Smith, W. S.; Hunt, A. N.; Jackowski, S. Modulation of CTP:phosphocholine cytidyltransferase by membrane curvature elastic stress. *Proc. Natl. Acad. Sci., U.S.A.* **2000**, *97* (16), 9032–9036.
- (33) Bezrukov, S. M. Functional consequences of lipid packing stress. *Curr. Opin. Colloid Interface Sci.* **2000**, *5* (3–4), 237–243.
- (34) Li, S.; Doyle, P.; Metz, S.; Royce, A. E.; Serajuddin, A. T. M. Effect of chloride ion on dissolution of different salt forms of haloperidol, a model basic drug. *J. Pharm. Sci.* **2005**, *94* (10), 2224–2231.
- (35) Li, S.; Wong, S.; Sethia, S.; Almoazen, H.; Joshi, Y. M.; Serajuddin, A. T. M. Investigation of Solubility and Dissolution of a Free Base and Two Different Salt Forms as a Function of pH. *Pharm. Res.* **2005**, *22* (4), 628–635.
- (36) Kunz, W.; Henle, J.; Ninham, B. W. Zur Lehre von der Wirkung der Salze (about the science of the effect of salts): Franz Hofmeister's historical papers. *Curr. Opin. Colloid Interface Sci.* **2004**, *9* (1–2), 19–37.
- (37) Gassim, A. E. H.; Girgis, Takla, P.; James, K. C. Polymorphism and possible intramolecular bonding in benperidol. *Int. J. Pharm.* **1986**, *34*, 1986.
- (38) Reed, L. L.; Schaefer, J. P. The Crystal and Molecular Structure of Haloperidol, a Patent Psychotropic Drug. *Acta Crystallogr., Sect. B: Struct. Sci.* **1973**, *29*, 1886.
- (39) Jakobsen, A. F.; Mouritsen, O. G.; Weiss, M. Close-up view of the modifications of fluid membranes due to phospholipase A2. *J. Phys.: Condens. Matter* **2005**, *17* (47), S4015.
- (40) Richieri, G. V.; Kleinfeld, A. M. Continuous Measurement of Phospholipase A2 Activity Using the Fluorescent Probe ADIFAB. *Anal. Biochem.* **1995**, *229* (2), 256–263.
- (41) Honger, T.; Jorgensen, K.; Stokes, D.; Biltonen, R. L.; Mouritsen, O. G.; Byron, R.; Edward, A. D. [9] Phospholipase A2 activity and physical properties of lipid-bilayer substrates. In *Methods Enzymology*, Vol. 286; Academic Press: New York, 1997; pp 168–190.
- (42) Leidy, C.; Linderth, L.; Andresen, T. L.; Mouritsen, O. G.; Jorgensen, K.; Peters, G. H. Domain-Induced Activation of Human Phospholipase A2 Type IIA: Local versus Global Lipid Composition. *Biophys. J.* **2006**, *90* (9), 3165–3175.
- (43) Nielsen, L. K.; Risbo, J.; Callisen, T. H.; Bjornholm, T. Lag-burst kinetics in phospholipase A2 hydrolysis of DPPC bilayers visualized by atomic force microscopy. *Biochim. Biophys. Acta* **1999**, *1420* (1–2), 266–271.
- (44) Hiraoka, M.; Abe, A.; Lu, Y.; Yang, K.; Han, X.; Gross, R. W.; Shayman, J. A. Lysosomal phospholipase A2 and phospholipidosis. *Mol. Cell. Biol.* **2006**, *26* (16), 6139–6148.
- (45) Kubo, M.; Hostetler, K. Y. Mechanism of cationic amphiphilic drug inhibition of purified lysosomal phospholipase A1. *Biochemistry* **1985**, *24* (23), 6515–6520.
- (46) von Berlepsch, H.; de Vries, R. Weakly charged lamellar bilayer system: Interplay between thermal undulations and electrostatic repulsion. *Eur. Phys. J. E* **2000**, *VI* (2), 141–152.

Received for review September 19, 2007

Revised manuscript received December 1, 2007

Accepted December 5, 2007

IE071265Q